

## High Pressure Study of Many-Particle Interactions at Metal-Insulator Transition in Low Dimensionality Electron Systems

*E. M. Dizhur\**, A.N.Voronovsky, M.A.Ill'ina, A.V.Fedorov,  
Institute for High Pressure Physics of RAS,

142190 Troitsk, Russia, dizhur@ns.hppi.troitsk.ru

I.N.Kotel'nikov, S.E. Dizhur, A.G. Zhuravlev, S.V. Zaitsev-Zotov  
Institute of Radioengineering and Electronics of the RAS,

125009 Moscow, Mokhovaya St. 11/7, Russia

**Summary.** We used the high pressure technique as an instrument in experimental studies of many-particle interactions in concern with the MIT in 2D electron system formed in Al/n-GaAs: $\delta$ (Si) structure as well as in NbS<sub>3</sub> that is an example of quasi-1D physical system with a collective electronic charge transport by a charge density wave. We report the results on the tunneling and the lateral conductance of 2DEG measured simultaneously at hydrostatic pressures in 2.5 GPa range at helium temperatures. The sharp resistivity rise along the  $\delta$ -doped layer shows that the MIT in 2DEG at about 2 Gpa is accompanied by significant evolution of many-particle interaction induced features (electron - LO-phonon and Zero Bias Anomaly due to the inter-electron interaction) in the tunneling spectra.

We observed also almost six orders resistivity drop of NbS<sub>3</sub>(I) at room temperature in a pressure range 3-6 GPa resulting in conductivity  $\sim 10^3 \text{ Ohm}^{-1}\text{cm}^{-1}$  comparable with that of other members of MX<sub>3</sub> family at room temperature. Being by two orders greater than the resistivity ratio of phases I and II of NbS<sub>3</sub> this transition cannot be attributed to a simple pressure-induced phase transition NbS<sub>3</sub> (I – II) and should rather be interpreted as pressure-induced insulator-metal transition in quasi-one dimensional conductor.

**Introduction.** The participation of many-particle interactions in determination of matter properties is now under rather extensive study. Apart from the strongly correlated systems where many-particle interactions are responsible for the phenomena like scirmions formation, a fractional quantum Hall effect, Wigner crystallization [1], exchange-correlation and/or electron-phonon interaction are known to appear also in metal-insulator transitions (MIT) [2], in weak localization effects [3] as well as in the tunneling [4]. In particular, the electron-phonon interaction is supposed to be responsible for fine features in the tunneling spectra of GaAs-based junctions at biases corresponding to the energy of LO-phonons, a peak-like singularity in the tunnel resistance, so called Zero Bias Anomaly (ZBA) is a consequence of the interelectron interaction in the plasma of a semiconductor [5].

When studying the many-particle interactions it is of importance to have the possibility of control over the carrier density. In semiconductors this is provided usually by the change of the doping level. However, not only the carrier density but also the scattering conditions change with doping so that it becomes difficult to separate the contribution of the carrier density and the scattering into the charge transport phenomena. Using the pressure in studies of the GaAs type semiconductors one can vary the carrier density in a wide range due to their capture by DX-centers the level of which may become resonant with the conduction band under pressure [6]. This gives a unique possibility to study the influence of the carrier density maintaining the static distribution of the impurities and structural defects over the sample practically invariable. The degree of disorder in the sample (that is responsible, in particular, for Mott-Anderson metal-insulator transition) obtained by the fabrication process, depends only on the magnitude of the potential fluctuations by the changeable charge state of the spatially fixed impurities and on screening by the free carriers with the changeable density. All above said looks like the reasonable ground for application of the high pressure technique as an instrument in studies of many-particle interactions.

In low-dimensional systems many-body interactions are more pronounced than in usual 3D-systems. In particular, dependence of Coulomb potential energy to kinetic energy ratio  $r_s$ , that measures the extent of non-ideality of electron gas, on electron density is more strong in lower dimensions. Besides, lowering the dimensionality of the system results in weaker screening thus increasing Coulomb energy even further.

In one-dimensional solids inter-electronic correlations are known to play a crucial role. Electronic properties of one-dimensional (1D) metals are known to be very different from those of three-dimensional (3D) metals well described by Landau's Fermi-liquid picture. In contrast to the 3D case, in purely 1D electronic system the Fermi-liquid picture breaks down and the single-electron quasiparticles do not exist. The only low energy excitations turn out to be charge and spin collective modes with the sound-like spectrum. Such a behavior has been given a generic name Luttinger liquid (for a review see [7]).

The case of a special interest is whether the Luttinger liquid can exist in quasi-1D conductors, i. e., highly anisotropic 3D solids with chain-like structure. Many-particle interactions play a significant role in these materials as well. The electron-phonon interaction in quasi-1D conductors leads to the Peierls phase transition resulting in formation of the correlated charge density wave (CDW) state. If the electron-electron interaction dominates over the electron-phonon one then the spin-density wave (SDW) transition occurs. Motion of the CDW or the SDW driven by an external electric field gives rise to a collective mechanism of the electron transport [8]. Both static and dynamic properties of the CDW and the SDW conductors are strongly affected by the Coulomb interaction [9].

According to present understanding, the formation of Luttinger liquid in quasi-1D conductors, in contrast to purely 1D system, is problematic because of the instability towards 3D coupling in the presence of arbitrarily small interchain hopping. Recent theoretical analysis shows, however, that the Luttinger liquid phase in quasi-one-dimensional conductors can be stabilized by crystalline defects and can exist in a form of a collection of bounded Luttinger liquids [10]. Thus, inter-electron interaction in quasi-1D conductors is supposed to produce Luttinger liquid type state, provided that the coupling integral between the crystalline chains is smaller than typical confinement energy. The latter depends on the distance between the neighboring impurities in a single chain. As the coupling between the chains should increase under pressure due to decreasing inter-chain distance, the transition from the Luttinger liquid like state to the Fermi liquid state, either metallic or with broken symmetry (CDW), may be anticipated in doped quasi-1D samples. The further increase of coupling should, in turn, destroy CDW and produce 3D behavior. Therefore, we are planning to use pressure as a tool to change effective dimensionality of the system in order to check existing concepts of electronic structure and mechanisms of conductivity in Q1D conductors.

Here we report the results on the tunneling and lateral transport in 2D electron system formed in  $\delta$ -doped Al/GaAs:Si structure under pressure up to 2.5 GPa as well as the result of pilot experiment on NbS<sub>3</sub>, at room temperature in 8 GPa pressure range.

***n*-Al/GaAs: $\delta$ <sub>Si</sub>.** In contrast to the magnetoresistivity like measurements, tunneling allows to study not only the filled subbands, but also the empty ones. Recent studies of the pressure influence on the tunnel spectrum implied the possibility to reach the MIT in the 2DEG of  $\delta$ -doped layer [11]. The aim of this work is to extend the previous pressure range and to observe the MIT in 2DEG directly. The tunnel structures, shown in Fig.1, were fabricated in IRE RAS following the procedure described in [12]. On (100) GaAs substrate by the MBE method an undoped buffer layer with  $p \sim 5 \cdot 10^{15} \text{ cm}^{-3}$  was grown. The  $\delta$ -doped layer about 3 nm thick at the depth of 20 nm from Al/*n*-GaAs interface was formed at 570 C on the substrate containing  $5 \cdot 10^{12} \text{ cm}^{-2}$  Si atoms. At the final stage of growth cycle, an Al film 80 nm thick was deposited from the Knudsen cell in the same MBE chamber. Schematic structure and top view of the sample are shown on Fig. 1. Each of the samples had a pair of separate metal "gates" to provide tunnel current to the common  $\delta$ -layer (see Fig. 1, right). Photolithographically shaped tunnel junctions were supplied with Au-Ge-Ni alloy ohmic contacts to the  $\delta$ -layer.

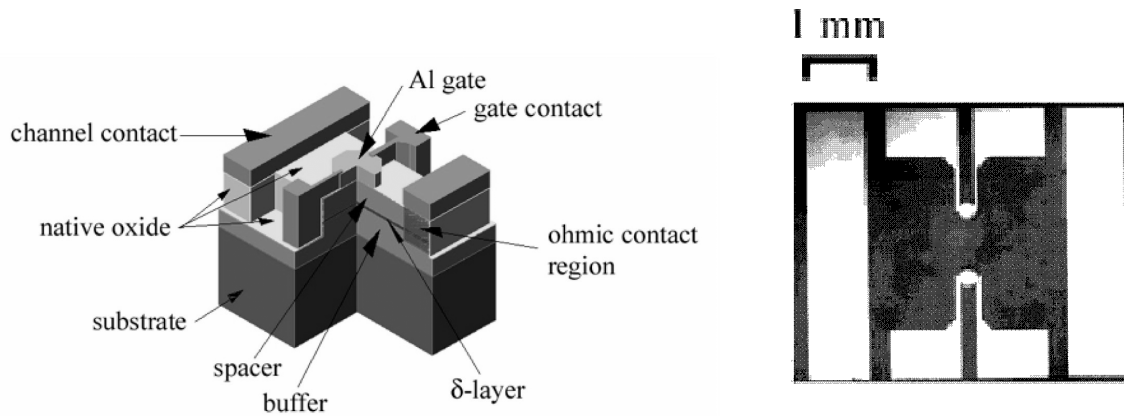


Figure 1: Schematic structure (left) and top view (right) of the sample Z1B7 [12]

In our studies we used a piston-cylinder clamp unit, developed in the IHPP of the RAS [13], that provides possibility of tunneling measurements in the pressure range up to 3 GPa at temperatures from 1.5 to 400 K. This piston-cylinder type unit is made of non-magnetic materials and uses polyethylene–siloxane neutral liquid as a pressure transmitting medium. The electric leads passing through the 0.8mm hole in the bottom plug are sealed by the Stycast epoxy.

The pressure is generated by loading the high pressure unit with a conventional laboratory press (up to 20 ton) using a manganine wire as a pressure gauge, the load is fixed and the unit is placed into the cryostat assembly. After the preliminary cooling down during the night with liquid nitrogen placed in the outer Dewar from room down to about 90K through the "soft" inner helium Dewar, no more than 3 litre of liquid helium was needed to cool the unit down to the liquid helium temperature 4.2 K. The pressure drop at cooling down was within 0.2 GPa and the actual value of the pressure during the measurements was evaluated (in GPa) by the change of the critical temperature  $T_c$  of the superconducting Sn wire placed *in situ* using the expression  $T_c = -0.495 P + 0.039 P^2$  [14].

Apart from direct measurements of the conductance of the 2D layer we were interested in obtaining tunneling data also. In the tunneling spectroscopy a current through the tunnel junction is measured versus the applied bias voltage. The commonly used way of retrieving tunnel spectra is based on modulation technique [15] when the sample is feeded with a DC bias with an addition of small AC component, so that the amplitudes of the 1st and 2nd harmonics of the modulation signal are proportional to the conductivity and its derivative with respect to the bias voltage respectively.

To overcome the difficulties due to high resistances both of the tunnelling junction and  $\delta$ -layer near the MIT, the alternative fully DC measurements of the tunnel current were carried out combined with proper mathematical treatment. The details of the circuitry that allow to measure the tunneling structures even with  $\sim 2\text{GOhm}$  tunneling resistance are described in [16].

In a common modulation technique, the compromise between resolution and signal-to-noise ratio is achieved by tuning the amplitude of the modulation voltage. Our approach includes two-stage smoothing  $I(V)$  presented in the tabular form using a smoothing cubic splines.

At the first stage the smoothing parameter was chosen so that to obtain the compromise between the noise and the clearness of the many-particle singularities at the second derivative of the spline using weight function inversely proportional to the previously obtained dispersions and "an eye judgement". At the second stage further smoothing was performed to separate the background reflecting the energy position of the quantum confinement subbands from the fine features due to the contribution of the many-particle interaction. This procedure is illustrated by the Fig.2.

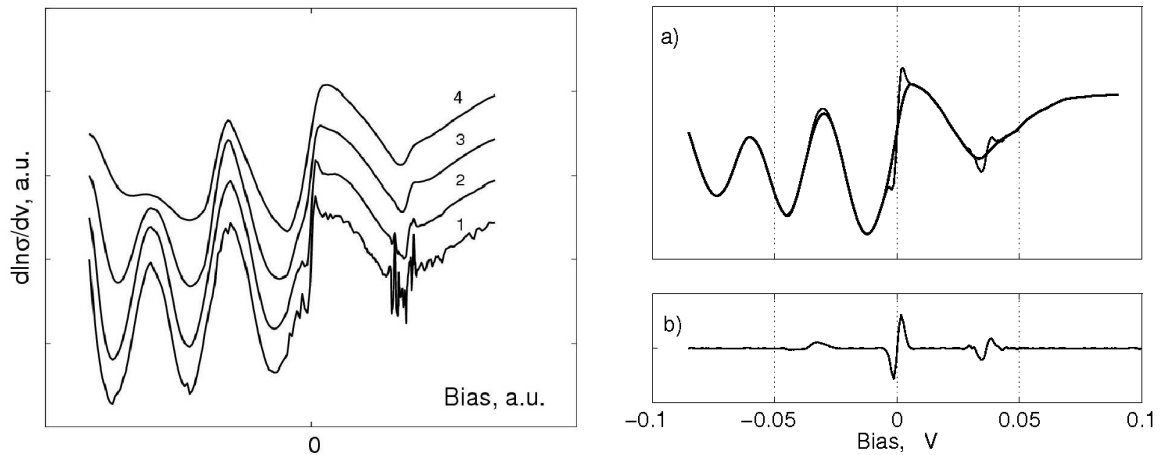


Figure 2: The calculated spectra  $d \ln \sigma / dV$  after successively increasing smoothing. The curve 2 is selected as the best one (left pane). Further smoothing (right pane) of the logarithmic derivative gives the background (a) and the many-particle features (b).

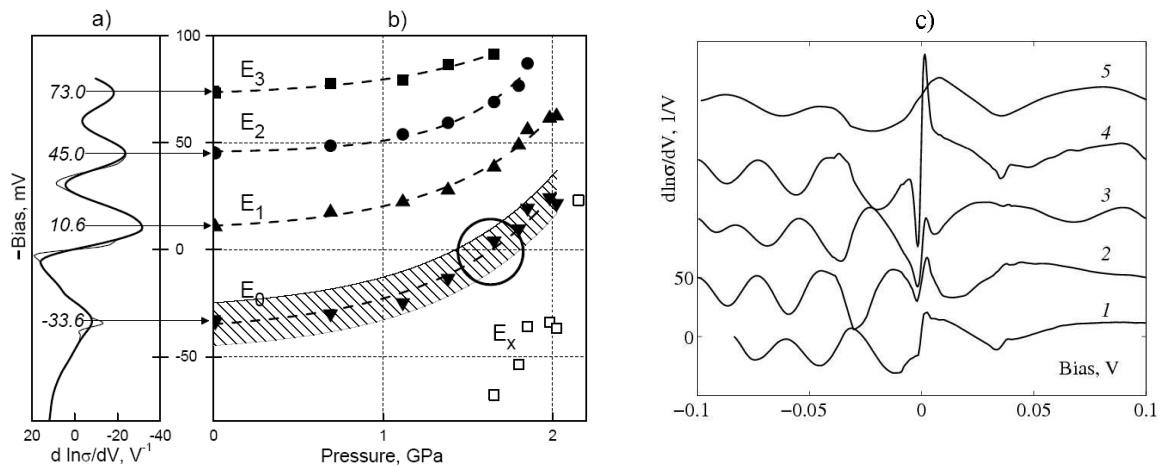


Figure 3: a) Tunneling spectrum (thin line) and its background (thick line) for sample Z1B7 at  $T = 4.2$  K,  $P=0$ . Arrows mark the positions of minima. b) Pressure dependence of the energies of the quantum-confinement 2D subbands. The patched area shows possible inhomogeneity of  $E_0$ . The circle marks MIT region. The empty boxes may be due to the band edge. The energies are referenced from the Fermi-level in the  $\delta$ -layer. c) Some spectra at different pressures: 1 -  $P=0$  GPa, 2 - 1.38, 3 - 1.66, 4 - 1.85, 5 - 2.02, each shifted by 50  $1/V$  vertically

The obtained data treated in the above way are presented on Figs.3-4. The background components of tunneling spectra measured at different pressures were used to find the movement of the 2D subbands under pressure (Fig.3a)<sup>1</sup>.

The behavior of many-particle features looks very complex. ZBA grows very sharply near the MIT and then drops to zero (Fig.3c). One should note that the pressure range where the ZBA has a narrow peak coincides with the onset of the fast lateral resistance growth and with the shoulder of tunneling resistance shown on Fig.4a. Apart from its physical sense we can conclude that the properties of the  $\delta$ -layer under the metal gate, reflected in the tunneling, do not differ very much from the rest, by far the larger, part of the  $\delta$ -layer under the free surface.

<sup>1</sup> Roughly speaking, the bias in V equals to the  $-(E-E_F)$ , eV

In the same pressure range the variation of the peak-to-valley width of the ZBA (Fig.4b) is observed as well as the drastic change of the thermal resistance coefficient of the lateral resistance (Fig.4c) – from  $\sim -0.03 \pm 0.02$  1/K in the range 0-1.8 GPa to  $\sim -4$  1/K at  $P = 2$  GPa, that is an additional evidence of the transition of the  $\delta$ -layer to the insulating state.

We believe that the transition of the  $\delta$ -layer to the insulating state is mainly due to the pressure induced changes in the energy-band structure of GaAs and, in particular, due to the presence of DX centers, which are characteristic of substitutional impurities (Sn, Si, Te) in  $A_3B_5$  semiconductors.

Fig.5 shows the potential distribution near the interface, which determines the number, position, and filling of quantum-confinement levels. In the case under consideration, as found from the selfconsistent solution of the Schrödinger and Poisson equations [11], at  $P = 0$  only one level  $E_0$  is located in the potential well below the Fermi level and the corresponding energy separation is  $E_0 - E_\Gamma = 92$ ,  $E_F - E_0 = 33$  meV.

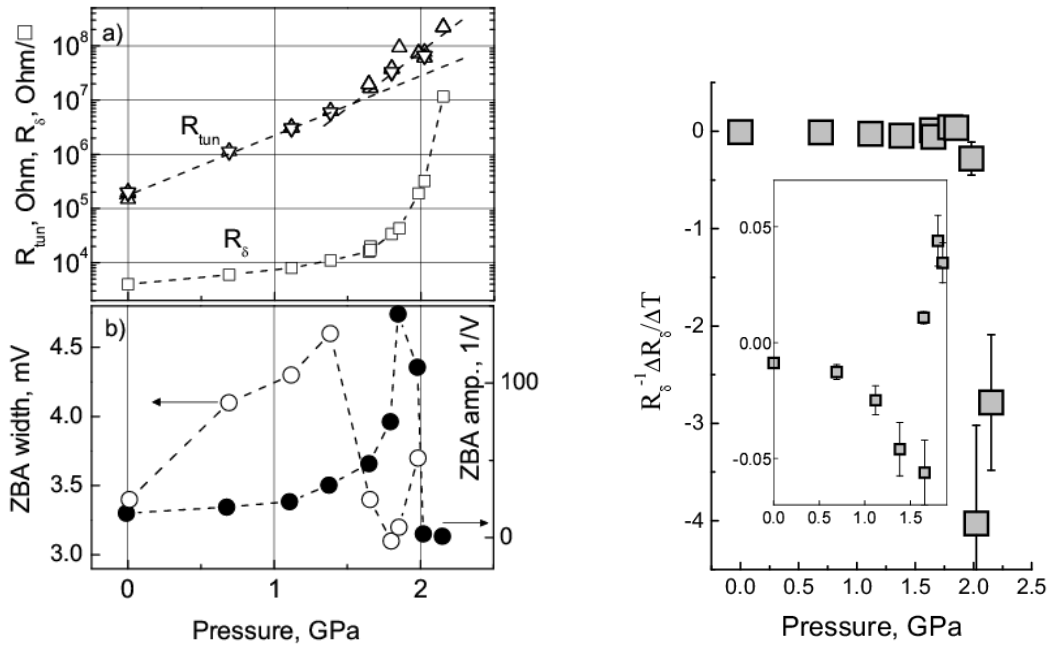


Figure 4: (a) Pressure dependence of the tunneling differential resistance  $R_{tun}$  at zero bias ( $\Delta$  – gate1,  $\nabla$  – gate2) and of the lateral resistance  $R_\delta$  ( $\square$ ) at  $T = 4.2$  K; (b) Pressure dependence of the ZBA peak-to-valley amplitude ( $\bullet$ ) and width ( $\circ$ ) at 4.2 K.; (c) Thermal coefficient  $\Delta(R_\delta)/\Delta(T)/R_\delta(4.2$  K) of the  $\delta$ -layer versus pressure. The inset zooms in the pre-MIT region.

According to the data of Maude et al. [17], at concentrations of Si close to the doping level of the  $\delta$ -layer in the samples studied here ( $4.5 \times 10^{12}$  cm $^{-2}$ ), the energy separation and its pressure derivative are  $E_{DX} - E_\Gamma = 270$  meV and  $dE_{DX-\Gamma}/dP = -94$  meV/GPa. As can be seen from the energy-band diagram Fig.5, the overlap of the Fermi level with the level of DX centers must begin at the pressure  $P_1 = [(E_{DX} - E_\Gamma) - (E_0 - E_\Gamma) - (E_F - E_0)]/|dE_{DX-\Gamma}/dP| = 1.65$  GPa. A further increase in the pressure leads to the Fermi level pinning and localization of carriers at DX centers, due to which the effective concentration of carriers involved in the charge transport over the  $\delta$ -layer gradually decreases. When the Fermi level shifts below the mobility threshold with respect to the quantum-confinement level, the transition to the insulating state occurs. The pressure range in which this transition is completed can be roughly estimated as  $P = (E_F - E_0) / |dE_{DX-\Gamma}/dP| = 0.35$  GPa, that is very close to the observed results.

The behavior of the tunnel resistance can be explained qualitatively as follows. Under pressure, the height of the tunnel barrier increases no faster than the band gap width – by  $\sim 100$  meV/GPa, (and even less for strongly degenerated systems as it was shown in [18]); the barrier width is determined mainly by the distance between the  $\delta$ -layer and the interface, i.e.,

changes insignificantly; and the density of states at the Fermi level for a 2D level changes as the effective mass, i.e., also insignificantly. Therefore, the general exponential character of the dependence of the tunnel current on bias undergoes no sharp changes at the transition to the insulating state. Nevertheless, the above factors still have some effect and the slope of the dependence  $\ln R(P)$  begins to change as soon as some part of free electrons is localized at DX centers, that leads to a change in the space charge in the  $\delta$ -layer as well. Because of the above mentioned broadening of the  $E_0$  level due to supposed inhomogeneity of the  $\delta$ -layer (and/or the barrier height) over the tunnel-contact area, the kink in the pressure dependence of the  $\ln R(P)$  shifts to somewhat lower pressures as compared with the above estimate. The main difference between the tunnel and lateral transport is that the former reflect the density of states and not the total carrier density.

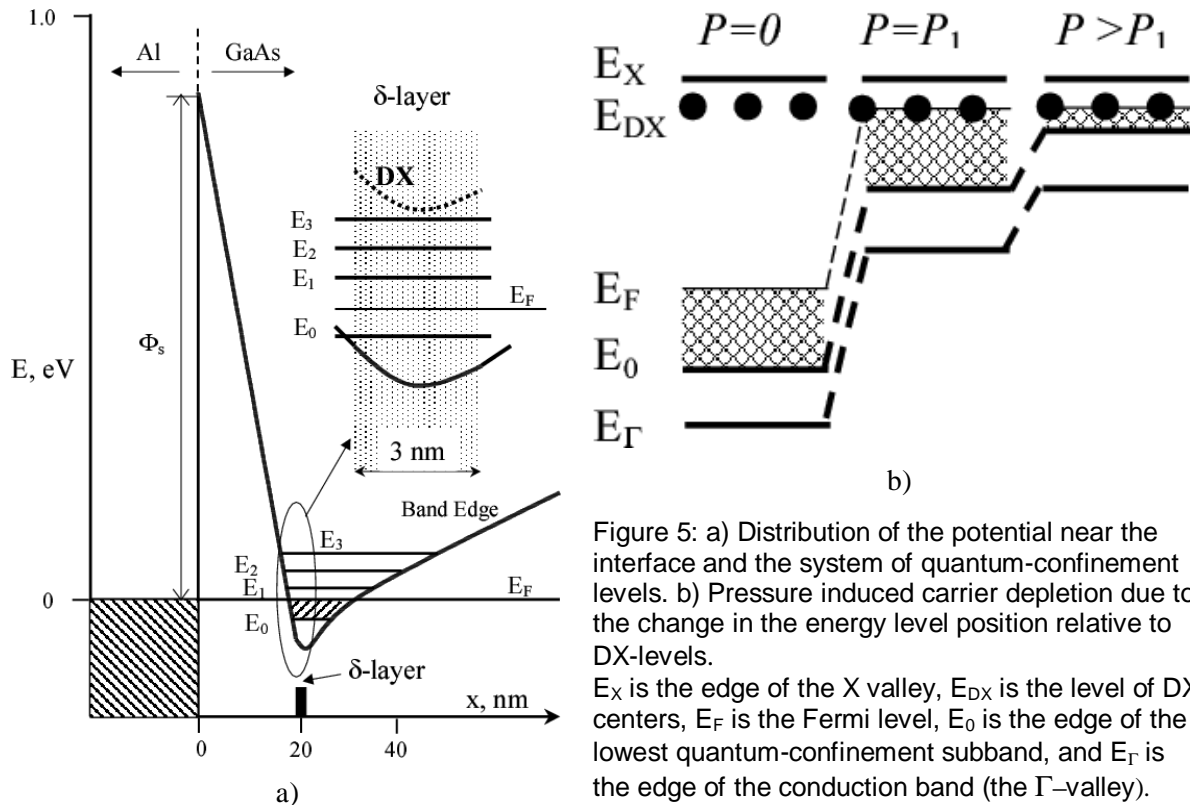


Figure 5: a) Distribution of the potential near the interface and the system of quantum-confinement levels. b) Pressure induced carrier depletion due to the change in the energy level position relative to DX-levels.

$E_X$  is the edge of the X valley,  $E_{DX}$  is the level of DX centers,  $E_F$  is the Fermi level,  $E_0$  is the edge of the lowest quantum-confinement subband, and  $E_\Gamma$  is the edge of the conduction band (the  $\Gamma$ -valley).

The behavior of the ZBA is less clear. On the one hand, this phenomenon was attributed to the effects of exchange-correlation interaction and the increase in the ZBA amplitude under pressure was predicted for three-dimensional systems [5]. On the other hand, the behavior of ZBA near the transition to the insulating state of the 2D system studied here may indicate, for example, the appearance of a Coulomb gap [19] in the spectrum, which, as is known, may manifest itself in tunneling [20]. In any case, the origin of a sharp peak in the baric dependence of the ZBA near the transition to the insulating state, the significant magnitude of this effect, and the nonmonotonic dependence of the ZBA width on pressure deserve to be carefully studied. Looking at the evident change of the effective width of this singularity (Fig.4a) it is not unreasonable to suppose that the nature of ZBA changes from correlation to Coulomb mechanism as far as electron system becomes under pressure more depleted and the screening decreases.

A puzzling experimental result is the observation of an additional minimum on the background of the tunneling spectrum shown on Fig.3b that appears in the investigated bias range at  $\sim 1.5$  GPa and quickly moves upwards with pressure. We have a strong temptation to ascribe it to the conduction band edge but its involving in the tunneling is unclear.

**NbS<sub>3</sub>.** NbS<sub>3</sub> is a relatively little-studied member of MX<sub>3</sub> family (M=Ta,Nb, X=S,Se) of q-1D conductors. The family has a chain-like structure schematically shown in Fig. 6a. The chains are formed by MX<sub>3</sub> tetrahedrons. The coupling along the chains is much stronger than in the perpendicular direction. Consequently, these materials are highly anisotropic conductors

with conduction anisotropy around 4 in TaSe<sub>3</sub>, 20 in NbSe<sub>3</sub>, 200 in TaS<sub>3</sub>. As a result, TaSe<sub>3</sub> retains its metallic properties down to the lowest temperature, NbSe<sub>3</sub> demonstrates an intermediate behavior with two Peierls transitions at  $T_{P1} = 145$  K and  $T_{P2} = 59$  K and metal-like low-temperature conduction. At room temperature all these materials have metal-like conductivity of order  $2\text{-}5 \times 10^3 \text{ Ohm}^{-1} \text{ cm}^{-1}$ , and orthorhombic TaS<sub>3</sub> is a Peierls conductor with the Peierls transition temperature 220 K, monoclinic TaS<sub>3</sub> has two transitions at  $T_{P1} = 240$  K and  $T_{P2} = 180$  K, both modifications being dielectric at low temperatures. The properties of NbS<sub>3</sub> are substantially different. There are three structure modifications of NbS<sub>3</sub>. The modification of our interest NbS<sub>3</sub>(I) has a dimerized monoclinic structure schematically shown in Fig. 6b. The Nb-Nb distances are 3.04 Å and 3.69 Å. Parameters of the monoclinic elementary cell are  $a = 4.963$  Å,  $b = 6.730$  Å,  $c = 9.144$  Å,  $\beta = 97.17^\circ$ . Unit cell contains two chains. This material demonstrates dielectric properties at room temperature. The room-temperature conductivity of this modification is  $1.2 \times 10^{-2} \text{ Ohm}^{-1} \text{ cm}^{-1}$ . For comparison, the room temperature conduction of NbS<sub>3</sub>(II) is three orders of magnitude higher.

Hydrostatic pressure effect was studied in NbSe<sub>3</sub> [21] and TaS<sub>3</sub> [22]<sup>2</sup>. Two-fold suppression of the Peierls transition temperature was observed in NbSe<sub>3</sub> at moderate pressure 0.7 GPa [21]. In contrast, some enhancement of the Peierls state (growth of the conduction activation energy at  $T < T_P$ ) was found in TaS<sub>3</sub> under the hydrostatic pressure 1.4 GPa [22]. Here we present the pilot results on the pressure influence on resistivity of NbS<sub>3</sub> (I) crystals.

We studied conduction of NbS<sub>3</sub>(I) crystals prepared by the standard transport reaction method [23]. The value of the room-temperature resistivity of our samples ( $\sim 100 \text{ Ohm cm}$ ) is close to the published value [24]. As it is seen from Fig. 7, the temperature dependencies of resistance, obtained by two- and four-terminal technique, follow approximately the activation law with the activation energy  $\Delta \approx 4400$  K, (dashed line in Fig. 7), varying within 10-15%. This value is close to the published data  $\Delta = 4400$  K [24] and  $\Delta = 3800$  K [25], proving that the samples under study are NbS<sub>3</sub>(I). A chamber with an effective support of the high pressure cell developed in the Institute for High Pressure Physics of RAS [26]<sup>3</sup> allows to obtain quasi-hydrostatic pressures in the range  $\sim 2\text{-}8$  GPa in a macroscopic volume using pyrophyllite as a pressure transmitting medium. Four copper wires  $\varnothing 0.16$  mm were used as an electric leads to the sample providing the two-wire measurements of the resistivity over an effective length  $\sim 1$  mm.

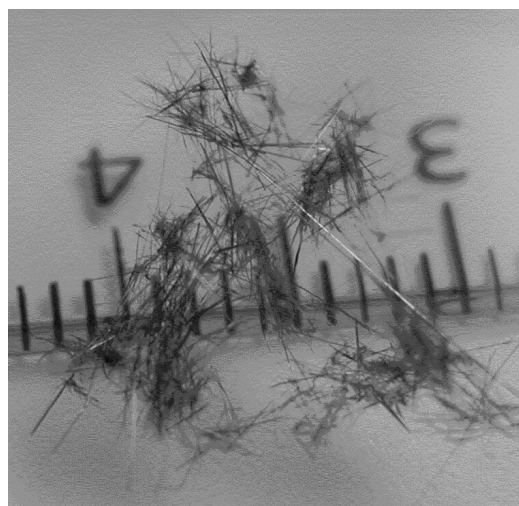
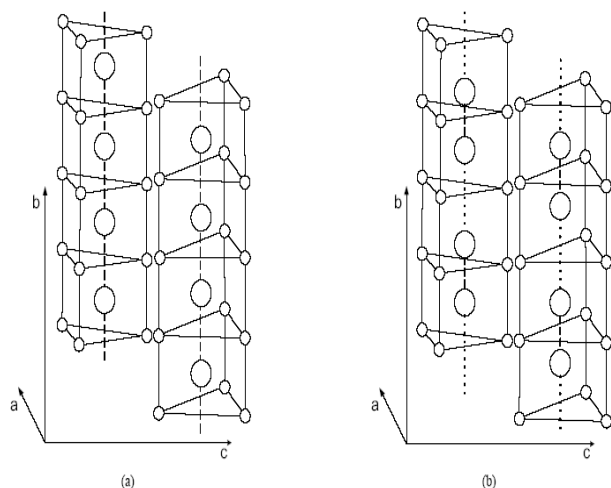


Figure 6: a) Schematic representation of a crystalline MX<sub>3</sub>-family structure. M – large ball, X – small balls; b) schematic representation of a crystalline NbS<sub>3</sub>(I) structure. Nb – large ball, S – small balls (left), and samples NbS<sub>3</sub> (right)

<sup>2</sup> Recently data on ZrSe<sub>3</sub> were reported in K Yamaya *et al.*, *J. Phys.: Condens. Matter* 14 10767-10770 (2002)

<sup>3</sup> often erroneously called "Paris - Edinburgh"

The results for 4 measured samples of NbS<sub>3</sub> are shown on Fig 8. We observed the 3 different types of pressure dependence of the resistance  $R(P)$ . Namely, the resistance of samples No.1 and No.4 was practically the same within an experimental accuracy, slowly decreasing (in logarithmic scale) up to ~ 4 GPa and sharply dropping down in the pressure range 4-5.5 GPa; the resistance of sample No.2 increased at the beginning and abruptly decreased at somewhat higher pressure range 5-7 GPa; sample No.3 had a tendency to increase in all the pressure range under study. When releasing the chamber the overall shape of the resistance corresponds to that in the loading run and was reversible within an experimental accuracy (inset in Fig. 8).

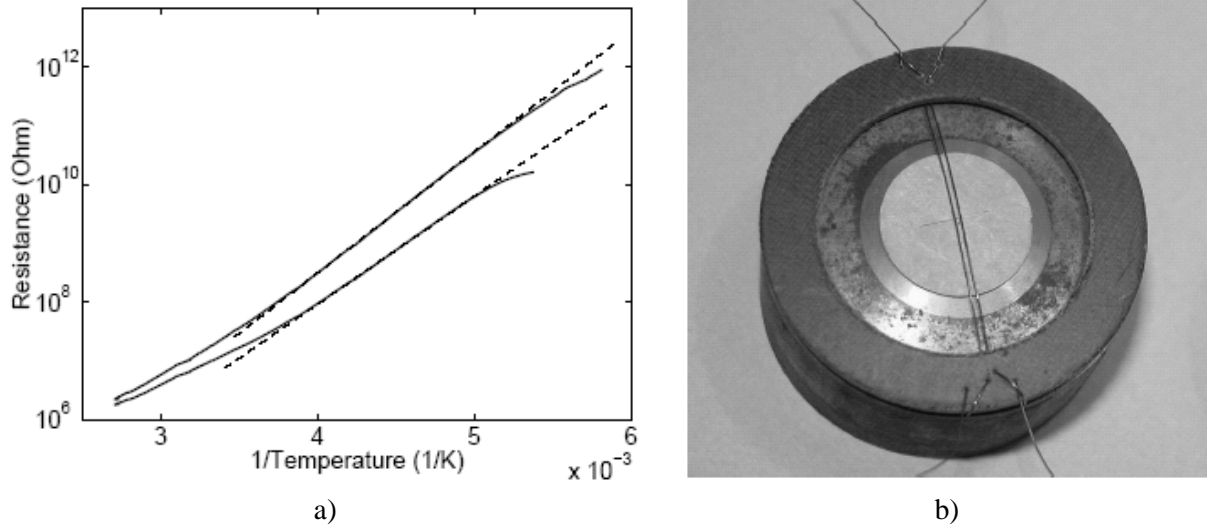


Figure 7: a) Typical temperature variation of resistivity of NbS<sub>3</sub>(l) sample (size is about 20x40x8000 nm), measured by two- and four- terminal technique (top and bottom curves, correspondingly). Dashed lines correspond to the activation law with the activation energy about 4400 K. b) High pressure cell assembly

The main result of our study is observation of almost 6 orders growth of conduction of NbS<sub>3</sub>(l) at room temperature in a pressure interval 4-7 GPa. The observed pressure induced resistance variation is almost three orders bigger than the resistivity ratio for NbS<sub>3</sub> phases I (commensurate) and II (incommensurate) ( $\rho_{(I)}/\rho_{(II)} \sim 10^3$ ), so that the observed transition is not a simple pressure-induced NbS<sub>3</sub>(I-II) phase transformation. At the same time, the high-pressure conductivity ( $\sim 10^3 \text{ Ohm}^{-1} \text{ cm}^{-1}$ ) is comparable with that of other members of MX<sub>3</sub> family at room temperature ( $2-5 \times 10^3 \text{ Ohm}^{-1} \text{ cm}^{-1}$ ). To our knowledge, the observed pressure-induced conduction variation is the biggest one among q-1D conductors.

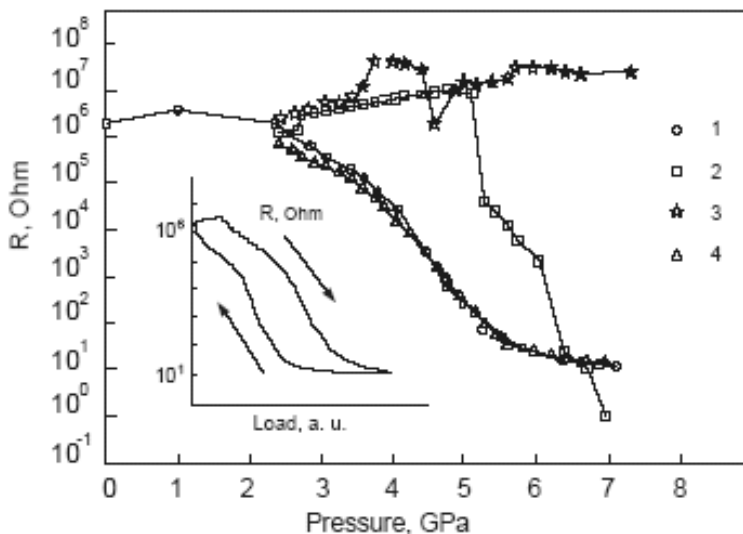


Figure 3: Pressure dependence of room temperature resistivity of 4 different samples; Inset represents resistance of sample No.1 during load and unload runs

At the same time, the observed behavior corresponds to general expectations for  $MX_3$  family compounds. The members of this compound may be ordered in accordance with their dimensionality in the following sequence:  $TaSe_3 \rightarrow NbSe_3 \rightarrow TaS_3 \rightarrow NbS_3$ . This sequence corresponds to increase of an effective inter-chain distance, decrease of inter-chain coupling, suppression of inter-chain hopping, i.e. growth of 1D effects in the direction  $TaSe_3 \rightarrow NbS_3$ . Application of pressure decreases the inter-chain distance and increases 3D effects, restoring thereby the metallic 3D conduction. While the general behavior of  $NbS_3(I)$  conduction under pressure seems to be understandable, a number of new questions arise. First of all, there is a question on the type of conductivity (metall-like or dielectric-like) under maximum pressure. There is also a question concerning the possibility to observe a transition from a very specific dimerized state intrinsic to  $NbS_3(I)$  (2-fold commensurability) to incommensurate CDW for intermediate pressure. These and many other questions will be addressed in our further study.

## Conclusion

The presented experimental matter may be outlined as follows:

- Pressure induced metal-insulator transition in the 2D electron system accompanied by the resistance growth by  $> 3$  orders of magnitude is reached in the GaAs tunnel structure with the near-to-surface Si doped  $\delta$ -layer that is confirmed by direct simultaneous measurements of tunneling and lateral transport.
- The obtained value of the MIT pressure  $\sim 1.9 \pm 0.2$  GPa is in quantitative accordance with the assumption that DX-centers are involved in the mechanism of carrier depletion under pressure.
- The properties of the  $\delta$ -layer are practically the same both under the metal gate and under the free surface.
- The thermal coefficient of the lateral resistivity changes from  $\sim -0.04$  before the MIT to  $\sim -4K^{-1}$  after the MIT.
- Almost 6 orders growth of conductivity of  $NbS_3(I)$  was observed at room temperature in a pressure interval 3-6 GPa.
- Conductivity of  $NbS_3(I)$  at the high-pressure side  $\gg 10^3 \text{ Ohm}^{-1} \text{ cm}^{-1}$  is comparable with that of others members of  $MX_3$  family.
- The observed transition is not a simple pressure induced  $NbS_3(I-II)$  phase transformation.

Acknowledgments. We are grateful to Ya. S. Savitskaya and V. V. Frolov for providing  $NbS_3$  samples. We acknowledge financial support by RFBR, INTAS, CRDF grants and by the programs "New materials and structures" and "Physics of compressed matter" of Physical Sciences Department of RAS. A part of these researches were performed in the frame of the CNRS-RAS-RFBR Associated European Laboratory "Physical properties of coherent electronic states in condensed matter" between CRTBT and IRE.

## References

- [1] S. Hikami, A. I. Larkin, and Y. Nagaoka, *Prog. Theor. Phys.* **63**, 707 (1980); S. Das Sarma and H. E. Hwang, *Phys. Rev. Lett.* **83**, 164 (1999); A. A. Abrikosov, *Fundamentals of the Theory of Metals*, North-Holland, Amsterdam (1988); A. Isihara, *Electron Liquids*, Springer-Verlag, Berlin (1997)
- [2] Y. Hanein, D. Shahar, et al., *Phys. Rev.* **B58**, R13338 (1998); B. L. Altshuler, D. L. Maslov, and V. M. Pudalov, *Physica E* **9**, 209 (2001)
- [3] S. V. Kravchenko, G. V. Kravchenko, J. E. Furneaux, et al. *Phys. Rev.* **B50**, 8039 (1994); G. Brunthaler, A. Prinz, G. Bauer, et al., *Ann.Phys.*, **8**, 579-584 (1999)
- [4] J. W. Conley and G. D. Mahan, *Phys. Rev.*, **161**, 681 (1967)
- [5] A. Ya. Shul'man, I. N. Kotel'nikov, N. A. Varvanin, et al. *JETP Lett.* **73**, 573 (2001)
- [6] J. G. Tischler, S. K. Singh, H. A. Nickel, et al., *phys. stat. sol. (b)* **211**, 131 (1998)

- [7] J. Voit, Rep. Prog. Phys. 58, 977 (1995)
- [8] For a review see: G. Gruner, *Density Waves in Solids*, Addison-Wesley, Reading, Massachusetts, 1994; P. Monceau, in: "*Electronic Properties of Inorganic Quasi-one-dimensional Conductors*", Part 2. , Ed. by P. Monceau, Dordrecht: D. Reidel Publ. Comp., 1985; S. V. Zaitsev-Zotov, *Physics: Uspechi*, 174(6), 585 (2004)
- [9] S.N. Artemenko and A.F. Volkov, Chapter 9 in "Charge Density Waves in Solids", edited by L. Gor'kov and G. Grüner, Elsevier Science, Amsterdam, 1989
- [10] S.N. Artemenko, JETP Letters, 79, 335(2004)
- [11] E. M. Dizhur, A. N. Voronovsky, I. N. Kotelnikov, *et al.*, *Phys. Stat. Sol.(b)*, **235**, 531 (2003)
- [12] I. N. Kotel'nikov, V. A. Kokin, Yu. V. Fedorov, *et al.*, *JETP Letters*, **71**, 387 (2000)
- [13] A. N. Voronovsky, E. S. Itskevich, E. M. Dizhur *et al.*, *Theses of the Conf. on "Advanced methods of pressure treatment"*, Chechoslovakia, Bratislava, 1982; <http://www.hppi.troitsk.ru>
- [14] L. D. Jennings, C. A. Swenson, *Phys. Rev.*, **112**, 31 (1958)
- [15] R. C. Jaklevic and J. Lambe, *Phys. Rev. Lett.* **17**, 1139 (1966)
- [16] E. M. Dizhur, A. V. Fedorov, <http://arxiv.org/list/cond-mat/0408206>
- [17] D. K. Maude, J. C. Portal, L. Dmowski, *et al*, *Solid State Phenomena*. **10**, 121-144 (1989)
- [18] E. M. Dizhur, A. Ya. Shul'man, I. N. Kotelnikov *et al.*, *Phys.Stat.Sol.(b)* **223**, 129 (2001)
- [19] B. I. Shklovskii and A. L. Efros, in *Electronic Properties of Doped Semiconductors (Nauka, Moscow, 1979; Springer, New York, 1984)*
- [20] J. G. Massey and Mark Lee, *Phys. Rev. Lett.* **75**, 4266 (1995); *Phys. Rev. Lett.* **77**, 3399 (1996)]
- [21] Syuma Yasuzuka, Yoshitoshi Okajima, *Phys. Rev. B* **60** 4406 (1999)
- [22] D. Moses, R. M. Boysel, *Phys. Rev. B* **31**, 3202 (1985)
- [23] Boswell F W and Prodan A 1980 *Physica* **99B** 361
- [24] Z. Z. Wang and P. Monceau, *Phys. Rev. B* **40**, 11589 (1989)
- [25] M. E. Itkis, F. Ya. Nad', S. V. Zaitsev-Zotov, *Solid State Commun.*, **71**, 895 (1989)
- [26] L. G. Khvostantsev *et al.*, *High Temp. {High Press.*, **9**(6), 637 (1977)